

Unsupervised Domain Adaptation for Semantic Segmentation via Low-level Edge Information Transfer

Hongruixuan Chen
Wuhan University
Wuhan, China
Qschr@whu.edu.cn

Yonghao Xu
Wuhan University
Wuhan, China
yonghaoxu@ieee.org

Chen Wu
Wuhan University
Wuhan, China
chen.wu@whu.edu.cn

Bo Du
Wuhan University
Wuhan, China
gunspace@163.com

ABSTRACT

Unsupervised domain adaptation for semantic segmentation aims to make models trained on synthetic data (source domain) adapt to real images (target domain). Previous feature-level adversarial learning methods only consider adapting models on the high-level semantic features. However, the large domain gap between source and target domains in the high-level semantic features makes accurate adaptation difficult. In this paper, we present the first attempt at explicitly using low-level edge information, which has a small inter-domain gap, to guide the transfer of semantic information. To this end, a semantic-edge domain adaptation architecture is proposed, which uses an independent edge stream to process edge information, thereby generating high-quality semantic boundaries over the target domain. Then, an edge consistency loss is presented to align target semantic predictions with produced semantic boundaries. Moreover, we further propose two entropy reweighting methods for semantic adversarial learning and self-supervised learning, respectively, which can further enhance the adaptation performance of our architecture. Comprehensive experiments on two UDA benchmark datasets demonstrate the superiority of our architecture compared with state-of-the-art methods.

CCS CONCEPTS

• Computing methodologies → Transfer learning; Image segmentation; Scene understanding.

KEYWORDS

unsupervised domain adaptation, transfer learning, semantic segmentation, edge information, convolutional neural networks

ACM Reference Format:

Hongruixuan Chen, Chen Wu, Yonghao Xu, and Bo Du. 2021. Unsupervised Domain Adaptation for Semantic Segmentation via Low-level Edge Information Transfer. In *Proceedings of -*. ACM, New York, NY, USA, 10 pages. <https://doi.org/x.xx/xxxx.xxxx>

1 INTRODUCTION

Semantic segmentation is a fundamental task in image processing, which aims to assign semantic labels to all pixels in a given image. Obtaining precise semantic segmentation results is significant for many vision-based applications [5, 33, 44, 46, 47, 55]. Nowadays, deep learning-based models, especially convolutional neural networks (CNNs) [21, 22], have achieved promising progress in semantic segmentation. To train a good segmentation network, a large number of fully annotated images are often required. Nevertheless, collecting large-scale datasets with accurate pixel-level annotation is time-consuming [9]. To reduce labeling consumption, an alternative way is utilizing synthetic images with precise pixel-level annotations to train the deep models. These synthetic images and corresponding annotations can be automatically generated by game engines, such as Grand Theft Auto V (GTAV) [34]. However, due to the large domain gap caused by the appearance difference between synthetic images and real images, the models trained on the synthetic images (source domain) inevitably face severe performance degradation on the real-world image datasets (target domain).

To address this issue, unsupervised domain adaptation (UDA) methods have been introduced to reduce the domain gap between labeled source domain and unlabeled target domain. In terms of the semantic segmentation task, adversarial learning-based UDA approaches demonstrate good efficiency in aligning domain gaps in the feature-level [15, 31, 38, 41, 51]. All of these methods align high-level feature distributions of different domains since high-level features contain abundant semantic category information. However, the large inter-domain gap in the high-level semantic representations makes the accurate alignment difficult. As pointed by Luo *et al.* [31], directly aligning the high-level semantic features may lead to negative transfer and damage the adaptation performance in the originally well-aligned regions. To address this issue, they propose a local score alignment map to guide the transfer of semantic information.

Permission to make digital or hard copies of all or part of this work for personal or classroom use is granted without fee provided that copies are not made or distributed for profit or commercial advantage and that copies bear this notice and the full citation on the first page. Copyrights for components of this work owned by others than ACM must be honored. Abstracting with credit is permitted. To copy otherwise, or republish, to post on servers or to redistribute to lists, requires prior specific permission and/or a fee. Request permissions from permissions@acm.org.

-, -, -

© 2021 Association for Computing Machinery.

ACM ISBN -...\$-

<https://doi.org/x.xx/xxxx.xxxx>

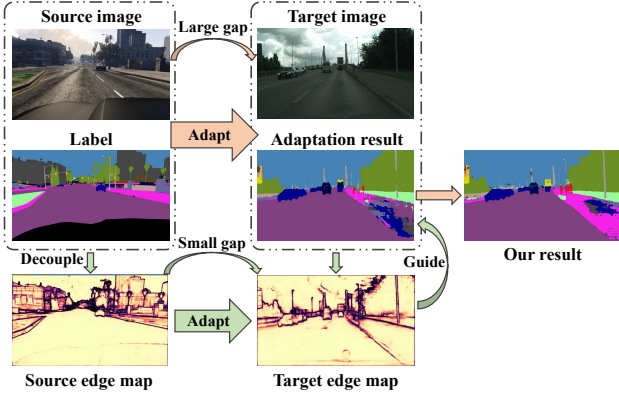


Figure 1: We propose to explicitly use low-level edge information with a small inter-domain gap for UDA in semantic segmentation. Compared with high-level semantic information, low-level edge information is easier to adapt; thus high-quality edge maps can be produced over the target domain. Since the edge information can reflect the boundaries of semantic category, it can be used to guide the transfer of semantic information.

In this paper, we provide a different viewpoint for addressing this issue. As argued in [30], in contrast to deep feature representations with large domain gaps and poor transferability, feature representations extracted by shallow convolutional layers are often general. Then, according to the visualization results of CNN reported in [52], the feature representations extracted by CNN show strong hierarchical nature and the shallow layers highly respond to low-level edge and color information. Based on these arguments and observations, we argue that low-level edge feature representations have a smaller inter-domain gap in comparison with high-level semantic features. Intuitively, it could be also observed that although the synthetic image and real-world image are quite different in appearance, the object shapes of the same category are very similar. Moreover, there exists a strong interaction between the edge information and the semantic information: the edge information can reflect the boundaries of semantic category.

Consequently, as shown in Figure 1, we treat low-level edge information as the transferable factor that could be used to facilitate transfer for high-level semantic information. Specifically, we present a semantic-edge domain adaptation (SEDA) architecture consisting of a semantic stream and an edge stream. In our architecture, the edge information is decoupled from the mainstream semantic network and is explicitly processed by an independent stream. The semantic stream adopts the existing entropy adversarial learning method as the basis. To better adapt hard target images, we present an entropy reweighting method to assign larger weights to harder images. For edge stream, we train it with the source semantic boundaries and adapt the source and target edge features through adversarial learning. An edge consistency loss function is applied to encourage the semantic segmentation predictions to correctly align with the semantic boundaries. As the target results with more accurate boundaries are obtained, we use self-supervised learning

(SL) to further fit the distribution of target domain. Furthermore, to overcome the issues of standard self-supervised learning, an uncertainty-adaptive self-supervised learning (UASL) is presented. The contributions of our work can be concluded as follows:

- (1) This paper proposes a semantic-edge domain adaptation architecture, which presents the first attempt at explicitly using edge information that has a small inter-domain gap for facilitating the transfer of high-level semantic information.
- (2) Two entropy-based reweighting methods are proposed to improve adversarial learning and self-supervised learning, enabling our architecture to learn better domain-invariant representations.
- (3) Experiments on two challenging benchmark adaptation tasks demonstrate that the proposed method can obtain better results than existing state-of-the-art methods.

2 RELATED WORK

2.1 Semantic Segmentation

Semantic segmentation is one of the most challenging computer vision tasks, which aims to predict pixel-level semantic labels for a given image. Following the work in [29], it has become mainstream to use fully convolutional network (FCN) architecture for tackling the semantic segmentation task, and many effective models have been presented [1, 7, 12, 28, 45, 47, 56]. Besides, some probability graph models like conditional random field [20] are used as an effective post-processing method for improving performance. More recently, some work introduces multi-task learning into semantic segmentation [6, 10, 19, 37], which combines networks for complementary tasks to improve semantic segmentation accuracy. Nevertheless, to train these semantic segmentation models, numerous real-world images with pixel-level annotations are required, which are usually difficult to collect. An alternative way is to train these models with photo-realistic synthetic data.

2.2 UDA for Semantic Segmentation

Unsupervised domain adaptation aims to align the domain distribution shift between labeled source data and unlabeled target data [4, 17, 25, 58, 59]. A very attractive application of UDA is using photo-realistic synthetic data to train semantic segmentation models, and a variety of methods have been presented, which can be broadly divided into three types: adversarial learning based approach [15, 18, 26, 38, 39, 41, 43], image translation approach [8, 14, 26, 50, 54], and self-supervised learning approach [8, 27, 36, 48, 53, 60].

Adversarial learning methods involve two networks. A generative network predicts the segmentation maps for the input source or target images. Another discriminator network takes the feature maps from generative network and tries to predict the domain type of feature maps, while generative network tries to fool the discriminator. By iteratively repeating this process, the two domains would have a similar distribution. In [15], the adversarial approach for first applied to UDA for semantic segmentation. In [41], adversarial learning is performed to match the entropy maps of two domains. In [31], a local alignment score map is designed to evaluate the category-level alignment degree for guiding the

transfer of semantic features. In [51], an attention-based discriminator network is presented to adaptively measure the hard-adapted semantic features.

Image translation methods directly apply adversarial models or style transfer approaches to transform the source images into target-style images for aligning the domain gap. In [14], CycleGAN [57] is used to transform the synthetic images of the source domain to the style of the target images. In [54], a style transfer network is presented to make the images from two domains visually similar. Recently, Yang *et al.* [50] use fast Fourier transform to reduce the appearance difference between images from different domains.

Self-supervised learning is another effective UDA approach. In the field of UDA for semantic segmentation, self-supervised learning methods use the target prediction as pseudo-labels to train the segmentation network, which could make the model implicitly learn the domain-invariant representations [51, 60]. In [60], a class balancing strategy and spatial prior are presented to guide the self-supervised learning in target domain. In [27], a pyramid curriculum strategy based on multi-scale pooling is proposed to select reliable pseudo-labels to train the segmentation network. Moreover, self-supervised learning could be combined with adversarial learning or image translation to further boost UDA performance [18, 32, 50, 51].

In this paper, unlike the previous adversarial learning methods that only focus on aligning the high-level semantic features, the proposed method simultaneously aligns semantic and edge features and utilizes adapted edge features to facilitate the transfer of semantic features. Moreover, we further present an entropy reweighting semantic adversarial learning strategy and an uncertainty-adaptive self-supervised learning approach to enhance the UDA performance.

3 METHODOLOGY

In UDA for semantic segmentation, the labeled source domain is denoted as $\mathcal{D}_S = \{(X_s, Y_s)\}_{s \in S}$, and the unlabeled target domain is denoted as $\mathcal{D}_T = \{X_t\}_{t \in T}$, where $X_s \in \mathbb{R}^{H \times W \times 3}$ is a source image, $Y_s \in \mathbb{R}^{H \times W \times C}$ is the one-hot semantic label associated with X_s , and $X_t \in \mathbb{R}^{H \times W \times 3}$ is a target image. Our goal is to utilize the low-level edge information, which is relatively easier to be transferred on the two domains, to guide the semantic segmentation over the target domain, thereby obtaining desirable prediction performance. Figure 2 illustrates our architecture that mainly contains three parts: semantic information transfer, edge information transfer, and uncertainty-adaptive self-supervised learning.

3.1 Semantic Information Transfer

Semantic stream G_{sem} is the basis of our architecture. Specifically, we use entropy adversarial learning method as our baseline, which has yielded promising results in UDA for semantic segmentation [41] and has served as the basis of more advanced methods [32, 42]. First, G_{sem} is trained by minimizing cross-entropy loss \mathcal{L}_{sem}^{seg} over source data:

$$\mathcal{L}_{sem}^{seg} = - \sum_{h,w} \sum_c Y_s^{(h,w,c)} \log P_s^{(h,w,c)} \quad (1)$$

where $P_s \in \mathbb{R}^{H \times W \times C}$ is the source semantic prediction map generated by G_{sem} . Besides, to overcome the negative effect of class

imbalance problem, Lovász-softmax loss [3] is imposed on source data.

Subsequently, G_{sem} takes a target image as input and outputs the semantic prediction map P_t . Then, the weighted self-information map $I_t \in \mathbb{R}^{H \times W \times C}$ is calculated:

$$I_t^{(h,w)} = -P_t^{(h,w)} \log P_t^{(h,w)} \quad (2)$$

To reduce the domain gap, in entropy adversarial learning, a discriminator D_{sem} is trained to predict the domain type for the weighted self-information map, and G_{sem} is trained to fool D_{sem} . However, the entropy adversarial learning treats all the target images equally, but there exist easy-adapt images with simple scenes and hard-adapt images with difficult scenes in the target domain. To better optimize these hard-adapt samples, we argue that harder samples need to contribute more loss during the training stage. Since the entropy map can reflect the confidence levels of the target predictions [41], we utilize the pixel-wise sum of target entropy map to measure the difficulty for each target image:

$$\begin{cases} E_t^{(h,w)} = -\frac{1}{\log C} \sum_c P_t^{(h,w,c)} \log P_t^{(h,w,c)} \\ \mathcal{E}_t = \sum_{h,w} E_t^{(h,w)} \end{cases} \quad (3)$$

where \mathcal{E}_t is the pixel-wise sum of entropy map E_t . If a target image has a low overall entropy value, it can be regarded as an easy-adapt sample, otherwise it is a hard-adapt sample. Based on this assumption, we propose an entropy reweighting adversarial loss:

$$\begin{aligned} \mathcal{L}_{sem}^{adv} = & - \sum_{h,w} \log (1 - D_{sem}(I_s)) \\ & - \left(1 + (\alpha \mathcal{E}_t)^2\right) \sum_{h,w} \log (D_{sem}(I_t)) \end{aligned} \quad (4)$$

where I_s is the source weighted self-information map, and α is a weight factor. Noteworthy, we adopt the square of entropy to enlarge the loss difference between easy-adapt samples and hard-adapt samples.

Through optimizing \mathcal{L}_{sem}^{seg} and \mathcal{L}_{sem}^{adv} , the two domains are aligned at the semantic feature maps to some extent. Next, we explicitly use the low-level edge information to further facilitate the transfer of semantic features.

3.2 Edge Information Transfer

In previous methods, edge information is entangled with other types of information in the segmentation network and is implicitly adapted through adversarial learning, which makes it difficult to use edge information for facilitating the transfer of semantic information.

To explicitly use low-level edge information, we use an independent edge stream G_{eg} to decouple edge information from G_{sem} . In terms of the specific network architecture, we adopt a lightweight auxiliary network introduced in [37] for edge detection. A gated convolutional layer is introduced in G_{eg} to ensure that G_{eg} only processes edge-relevant information. Specifically, G_{eg} takes the output of the first convolutional layer of G_{sem} as input and aims to yield precise semantic boundary maps \mathcal{B}_s and \mathcal{B}_t . To this end, G_{eg} is first trained by minimizing binary cross-entropy loss \mathcal{L}_{eg}^{seg}

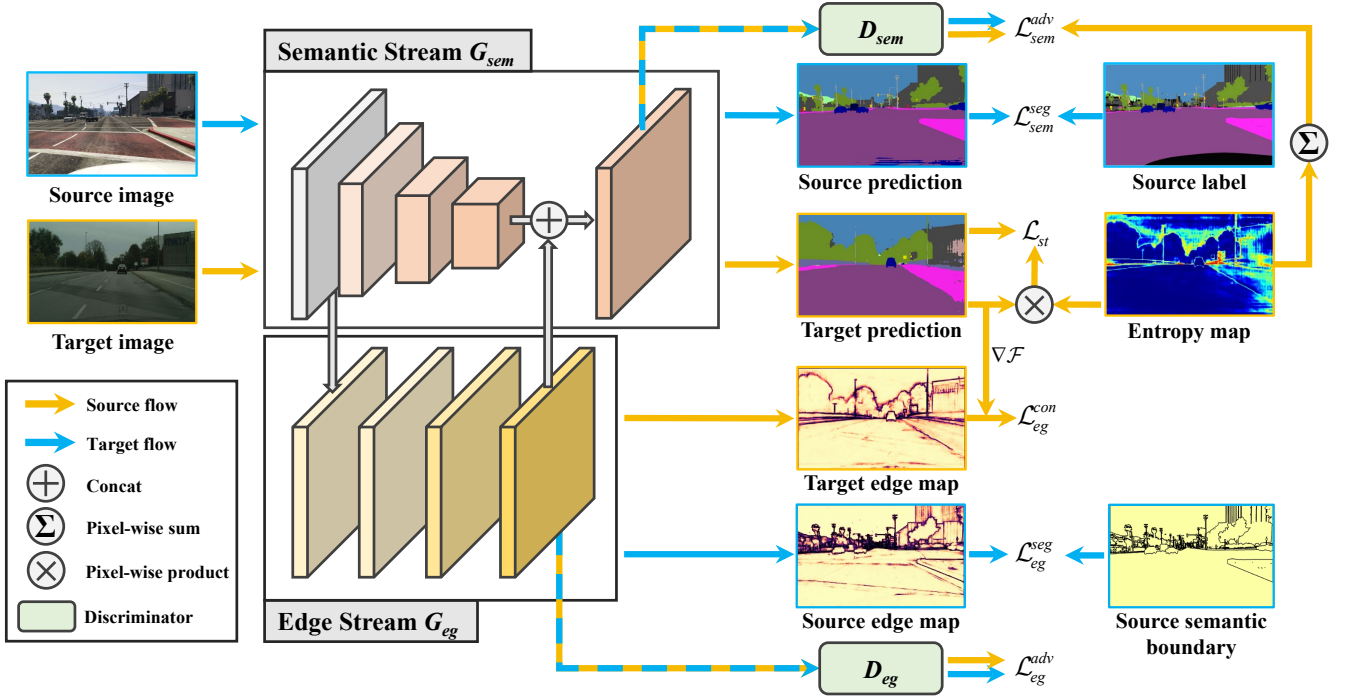


Figure 2: The overall architecture of our SEDA architecture, which composed of three parts: 1) In semantic information transfer, the feature-level adversarial learning approach is applied to align the semantic distributions of source and target domains. Besides, the entropy map of target output is utilized to weight each target sample at the image-level; 2) In edge information transfer, the edge information is decoupled from G_{sem} and independently processed by G_{eg} . Feature-level adversarial learning is also performed to align edge feature distributions of two domains. Then, the target semantic boundary map is used to guide the target semantic segmentation; 3) In uncertainty-adaptive self-supervised learning, the target prediction is weighted by entropy map at pixel-level and treated as pseudo-labels to train G_{sem} .

over the source domain. Ground truth of semantic boundaries can be directly generated from source semantic labels.

Through optimizing \mathcal{L}_{eg}^{seg} , G_{eg} is capable of generating precise semantic boundaries for source domain data. Compared to high-level semantic features, the low-level edge features have a smaller domain gap. Moreover, due to optimizing \mathcal{L}_{sem}^{adv} , the inter-domain gap in the features of shallow layers is further reduced. Accordingly, despite merely supervised by source edge information, G_{eg} can generate decent boundaries in the target domain. To produce higher quality semantic boundaries for target domain, similar to semantic stream, we also introduce a discriminator D_{eg} for predicting the domain labels for the edge feature maps, while G_{eg} is trained to fool D_{eg} :

$$\mathcal{L}_{eg}^{adv} = - \sum_{h,w} (\log(1 - D_{eg}(\mathcal{H}_s)) + \log(D_{eg}(\mathcal{H}_t))) \quad (5)$$

where \mathcal{H}_s and \mathcal{H}_t are the edge features of source and target domains from the last layer of G_{eg} .

Subsequently, we add the target edge feature map back to G_{sem} , thereby guiding the semantic segmentation over the target domain. However, this way can only implicitly refine the semantic segmentation results, which cannot guarantee consistency between the boundary map and the predicted semantic segmentation map. To

explicitly encourage the target semantic segmentation maps to align with the boundary map, we introduce an edge consistency loss \mathcal{L}_{eg}^{con} :

$$\begin{cases} \mathcal{P}_t = \frac{1}{\sqrt{2}} \left\| \nabla \left(\mathcal{F} * \arg \max_c P_t \right) \right\| \\ \mathcal{L}_{eg}^{con} = \sum_{N^+} \left| \mathcal{P}_t^{(N^+)} - \mathcal{B}_t^{(N^+)} \right| \end{cases} \quad (6)$$

where \mathcal{P}_t is the semantic boundary map computed by taking a spatial derivative on the target segmentation output, \mathcal{F} is Gaussian filter, and N^+ contains coordinates of all boundary pixels in both \mathcal{P}_t and \mathcal{B}_t .

\mathcal{L}_{eg}^{con} aims at ensuring that target semantic boundary pixels are penalized if there is a mismatch with boundaries predicted by G_{eg} . By optimizing \mathcal{L}_{eg}^{con} , G_{sem} can be guided by the target boundary map, thereby generating more accurate target prediction map. Furthermore, since argmax operator is not differentiable, the Gumbel softmax trick [16] is adopted to approximate the partial derivatives of \mathcal{L}_{eg}^{con} to a given parameter during the backward propagation stage.

3.3 Uncertainty-Adaptive Self-Supervised Learning

By means of using the low-level edge information to guide the transfer of semantic information, G_{sem} can generate more accurate semantic segmentation results over the target domain. Subsequently, considering the complex distribution of real-world data (target domain), we apply the self-supervised learning strategy to make our architecture further fit the distribution of the target domain.

The standard self-supervised learning method [32, 60] sets a threshold to select high-confident target pseudo-labels. However, it is difficult to choose a suitable threshold: an over-large threshold could make the available target information very less, and an over-small threshold could produce too many noisy labels, damaging the adaptation performance. Besides, the confidence levels of these selected pseudo-labels are also different. To address these issues, we present an uncertainty-adaptive self-supervised loss that adopts entropy to adaptively estimate uncertainty and reweight target prediction at pixel-level:

$$\mathcal{L}_{uasl} = - \sum_{h,w} \left(1 - E_t^{(h,w)}\right)^2 \sum_c \hat{Y}_t^{(h,w,c)} \log P_t^{(h,w,c)} \quad (7)$$

where \hat{Y}_t is the one-hot semantic pseudo-labels.

Both \mathcal{L}_{sem}^{adv} and \mathcal{L}_{uasl} adopt entropy to measure uncertainty and reweight samples. However, \mathcal{L}_{sem}^{adv} uses the sum of entropy to weight the target image at the image-level, but \mathcal{L}_{st} uses entropy map to weight target prediction at the pixel-level. In \mathcal{L}_{sem}^{adv} , the image with larger entropy means harder to adapt and is assigned more weight. In contrast, the pixel with a smaller entropy value represents higher confidence and is more highlighted in \mathcal{L}_{uasl} .

Finally, our complete loss function \mathcal{L} is formed by all the loss functions:

$$\mathcal{L} = \mathcal{L}_{sem}^{seg} + \lambda_1 \mathcal{L}_{sem}^{adv} + \lambda_2 \mathcal{L}_{eg}^{seg} + \lambda_3 \mathcal{L}_{eg}^{adv} + \mathcal{L}_{eg}^{con} + \mathcal{L}_{uasl} \quad (8)$$

where λ_1 to λ_3 are trade-off parameters that weight the importance of the corresponding terms. And our optimization objective is to learn a target model \mathcal{G} according to:

$$\mathcal{G} = \arg \min_{G_{sem}} \min_{G_{sem}} \max_{D_{sem}} \mathcal{L}_{D_{sem}} \quad (9)$$

The full training procedure of our method consists of three steps: 1) jointly optimizing G_{sem} , D_{sem} , G_{eg} , and D_{eg} by semantic segmentation loss, edge loss, and two adversarial learning loss over the source and target domains; 2) generating pseudo labels and correspond entropy maps by G_{sem} over the target domain; 3) optimizing G_{sem} by uncertainty-adaptive self-supervised loss.

4 EXPERIMENTS

In this section, following the common protocol of previous works [15, 31, 41], we conduct experiments on the two-challenging synthetic-to-real unsupervised domain adaptation tasks, i.e., GTAV→Cityscapes, and SYNTHIA→Cityscapes. Specifically, we use GTAV or SYNTHIA datasets with pixel-level annotations as the source domain and Cityscapes dataset without any annotations as the target domain.

4.1 Datasets

Cityscapes is a real-world urban scene image dataset, which provides 3975 images, each of which has a resolution of 2048×1024, collected from 50 cities in Germany [9]. Following the standard protocols [15, 31, 41], we use the 2975 images from Cityscapes dataset training set as the unlabeled target domain for training, and evaluate our method on the 500 images from the validation set.

GTAV is a large synthetic dataset containing 24966 high quality labeled urban scene images with a resolution of 1914×1052 from open-world computer games, Grand Theft Auto V [34]. The 19 compatible semantic classes between GTAV and Cityscapes are selected in the experiment.

SYNTHIA is another synthetic urban scene dataset [35]. Following previous works, we use the SUNTHIA-RAND-CITYSCAPES subset that contains 9400 annotated images with a resolution of 1280×760 and shares 16 semantic classes with Cityscapes. In the training stage, we consider the 16 common classes with the Cityscapes. In the evaluation stage, 16- and 13-class subsets are used to make quantitative assessment.

4.2 Implementation Details

All the experiments in this paper¹ are implemented with Pytorch in a single NVIDIA GTX 1080Ti GPU. Limited by the GPU memory, during the training stage, the resolution of Cityscapes images is resized to 1024×512, and that of GTAV images is resized to 1280×720. The resolution of SYNTHIA images remains unchanged. For the sake of fair comparison, like most of the state-of-the-art methods, we do not use any data augment technique.

For the semantic stream G_{sem} , following most of the state-of-the-art methods, we use ResNet-101 architecture [13] with pretrained parameters from ImageNet [11]. The implementation of edge stream G_{eg} follows the work [37]. G_{eg} is mainly composed of three residual blocks, and each block is followed by a gated convolutional layer, ensuring G_{eg} only processes edge related information. For the discriminator D_{sem} , we apply the same architecture used in [41]. For the discriminator D_{eg} , we adopt a simple structure consisting of three 4×4 convolutional layers with a stride of 2, and one 1×1 convolutional layer. Except for the last layer, each convolutional layer is followed by a Leaky-ReLU with a slope of 0.2.

To verify the robustness of our method, the hyper-parameters keep the same in both tasks. For our joint loss, the values of λ_1 to λ_3 are set as $1e^{-3}$, 20, and $1e^{-3}$, respectively. The weight factor α in entropy reweighting adversarial loss is set to 10. In terms of the whole architecture training, the SGD optimizer with a learning rate of $2.5e^{-4}$, momentum of 0.9, and a weight decay of $5e^{-4}$ is utilized to train G_{sem} and G_{eg} . Two Adam optimizers with a learning rate of $1e^{-4}$ are used for training D_{sem} and D_{eg} , respectively.

4.3 Performance Comparison

In this subsection, we compare our proposed method with the existing state-of-the-art methods [18, 23, 24, 26, 27, 31, 32, 38, 39, 41, 43, 49–51]. For the sake of fairness, all the reported methods use ResNet-101 as the backbone network and the data augment

¹The source code will be made publicly available.

Table 1: Evaluation results of semantic segmentation by adapting from GTAV to Cityscapes. The mechanism “T”, “A”, and “S” mean image translation, adversarial training, and self-supervised learning, respectively. The best results are highlighted in bold.

GTAV→Cityscapes																					
	Mech.	road	sidewalk	building	wall	fence	pole	light	sign	veg.	terrain	sky	person	rider	car	truck	bus	train	mbike	bike	mIoU
Methods																					
AdaSegNet [38]	A	86.5	36.0	79.9	23.4	23.3	23.9	35.2	14.8	83.4	33.3	75.6	58.5	27.6	73.7	32.5	35.4	3.9	30.1	28.1	42.4
ADVENT [41]	A	89.4	33.1	81.0	26.6	26.8	27.2	33.5	24.7	83.9	36.7	78.8	58.7	30.5	84.8	38.5	44.5	1.7	31.6	32.4	45.5
CLAN [31]	A	87.0	27.1	79.6	27.3	23.3	28.3	35.5	24.2	83.6	27.4	74.2	58.6	28.0	76.2	33.1	36.7	6.7	31.9	31.4	43.2
AdaptPatch [39]	A	92.3	51.9	82.1	29.2	25.1	24.5	33.8	33.0	82.4	32.8	82.2	58.6	27.2	84.3	33.4	46.3	2.2	29.5	32.3	46.5
PyCDA [27]	S	90.5	36.3	84.4	32.4	28.7	34.6	36.4	31.5	86.8	37.9	78.5	62.3	21.5	85.6	27.9	34.8	18.0	22.9	49.3	47.4
CCM [24]	S	93.5	57.6	84.6	39.3	24.1	25.2	35.0	17.3	85.0	40.6	86.5	58.7	28.7	85.8	49.0	56.4	5.4	31.9	43.2	49.9
FDA [50]	TS	92.5	53.3	82.4	26.5	27.6	36.4	40.6	38.9	82.3	39.8	78.0	62.6	34.4	84.9	34.1	53.1	16.9	27.7	46.4	50.4
IntraDA [32]	AS	90.6	37.1	82.6	30.1	19.1	29.5	32.4	20.6	85.7	40.5	79.7	58.7	31.1	86.3	31.5	48.3	0.0	30.2	35.8	46.3
FADA [43]	AS	91.0	50.6	86.0	43.4	29.8	36.8	43.4	25.0	86.8	38.3	87.4	64.4	38.0	85.2	31.6	46.1	6.5	25.4	37.1	50.1
DAST [51]	AS	92.2	49.0	84.3	36.5	28.9	33.9	38.8	28.4	84.9	41.6	83.2	60.0	28.7	87.2	45.0	45.3	7.4	33.8	32.8	49.6
BDL [26]	TAS	91.0	44.7	84.2	34.6	27.6	30.2	36.0	36.0	85.0	43.6	83.0	58.6	31.6	83.3	35.3	49.7	3.3	28.8	35.6	48.5
TIR [18]	TAS	92.9	55.0	85.3	34.2	31.1	34.9	40.7	34.0	85.2	40.1	87.1	61.0	31.1	82.5	32.3	42.9	0.3	36.4	46.1	50.2
LDR [49]	TAS	90.8	41.4	84.7	35.1	27.5	31.2	38.0	32.8	85.6	42.1	84.9	59.6	34.4	85.0	42.8	52.7	3.4	30.9	38.1	49.5
UDACT [23]	TAS	95.3	65.1	84.6	33.2	23.7	32.8	32.7	36.9	86.0	41.0	85.6	56.1	25.9	86.3	34.5	39.1	11.5	28.3	43.0	49.6
SourceOnly	-	64.6	27.3	76.9	19.1	21.1	27.0	32.1	18.5	81.2	14.5	72.4	55.4	21.6	62.9	29.4	8.4	2.4	24.2	35.0	36.5
Ours	AS	94.0	61.8	85.8	29.2	32.5	35.4	40.6	43.3	87.2	43.9	84.4	63.8	29.1	88.7	46.0	49.9	0.0	43.7	49.9	52.8

Table 2: Evaluation results of semantic segmentation by adapting from SYNTHIA to Cityscapes. The mechanism “T”, “A”, and “S” mean image translation, adversarial learning, and self-supervised learning, respectively. We show the mIoU (%) of the 13 classes (mIoU*) excluding classes with “*”. “-” represents the method does not report the corresponding experimental result. The best results are highlighted in bold.

SYNTHIA→Cityscapes																			
Methods	Mech.	road	sidewalk	building	wall*	fence*	pole*	light	sign	veg.	sky	person	rider	car	bus	mbike	bike	mIoU	mIoU*
AdaSegNet [38]	A	81.7	39.1	78.4	11.1	0.3	25.8	6.8	9.0	79.1	80.8	54.8	21.0	66.8	34.7	13.8	29.9	39.6	45.8
ADVENT [41]	A	85.6	42.2	79.7	8.7	0.4	25.9	5.4	8.1	80.4	84.1	57.9	23.8	73.3	36.4	14.2	33.0	41.2	48.0
CLAN [31]	A	81.3	37.0	80.1	-	-	-	16.1	13.7	78.2	81.5	53.4	21.2	73.0	32.9	22.6	30.7	-	47.8
AdaptPatch [39]	A	82.4	38.0	78.6	8.7	0.6	26.0	3.9	11.1	75.5	84.6	53.5	21.6	71.4	32.6	19.3	31.7	40.0	46.5
PyCDA [27]	S	75.5	30.9	83.3	20.8	0.7	32.7	27.3	33.5	84.7	85.0	64.1	25.4	85.0	45.2	21.2	32.0	46.7	53.3
CCM [24]	S	79.6	36.4	80.6	13.3	0.3	25.5	22.4	14.9	81.8	77.4	56.8	25.9	80.7	45.3	29.9	52.0	45.2	52.9
FDA [50]	TS	79.3	35.0	73.2	-	-	-	19.9	24.0	61.7	82.6	61.4	31.1	83.9	40.8	38.4	51.1	-	52.5
IntraDA [32]	AS	84.3	37.7	79.5	5.3	0.4	24.9	9.2	8.4	80.0	84.1	57.2	23.0	78.0	38.1	20.3	36.5	41.7	48.9
FADA [43]	AS	84.5	40.1	83.1	4.8	0.0	34.3	20.1	27.2	84.8	84.0	53.5	22.6	85.4	43.7	26.8	27.8	45.2	52.5
DAST [51]	AS	87.1	44.5	82.3	10.7	0.8	29.9	13.9	13.1	81.6	86.0	60.3	25.1	83.1	40.1	24.4	40.5	45.2	52.5
BDL [26]	TAS	86.0	46.7	80.3	-	-	-	14.1	11.6	79.2	81.3	54.1	27.9	73.7	42.2	25.7	45.3	-	51.4
TIR [50]	TAS	92.6	53.2	79.2	-	-	-	1.6	7.5	78.6	84.4	52.6	20.0	82.1	34.8	14.6	39.4	-	49.3
LDR [49]	TAS	85.1	44.5	81.0	-	-	-	16.4	15.2	80.1	84.8	59.4	31.9	73.2	41.0	32.6	44.7	-	53.1
UDACT [23]	TAS	93.3	54.0	81.3	14.3	0.7	28.8	21.3	22.8	82.6	83.3	57.7	22.8	83.4	30.7	20.2	47.2	46.5	53.9
SourceOnly	-	55.9	22.7	72.1	9.3	0.1	24.7	10.3	10.4	73.8	77.9	54.9	20.5	41.2	31.7	8.3	11.5	32.8	37.8
Ours	AS	92.0	53.9	82.0	10.1	0.2	32.8	13.3	26.0	83.6	84.4	63.0	21.4	86.7	46.8	24.7	49.0	48.1	55.9

technique is not used. The per-class Intersection-Over-Union (IoU) and mean IoU (mIoU) are adopted as the evaluation criteria.

GTAV to Cityscapes. Table 1 displays the comparison results from GTAV to Cityscapes. First, all domain adaptation methods

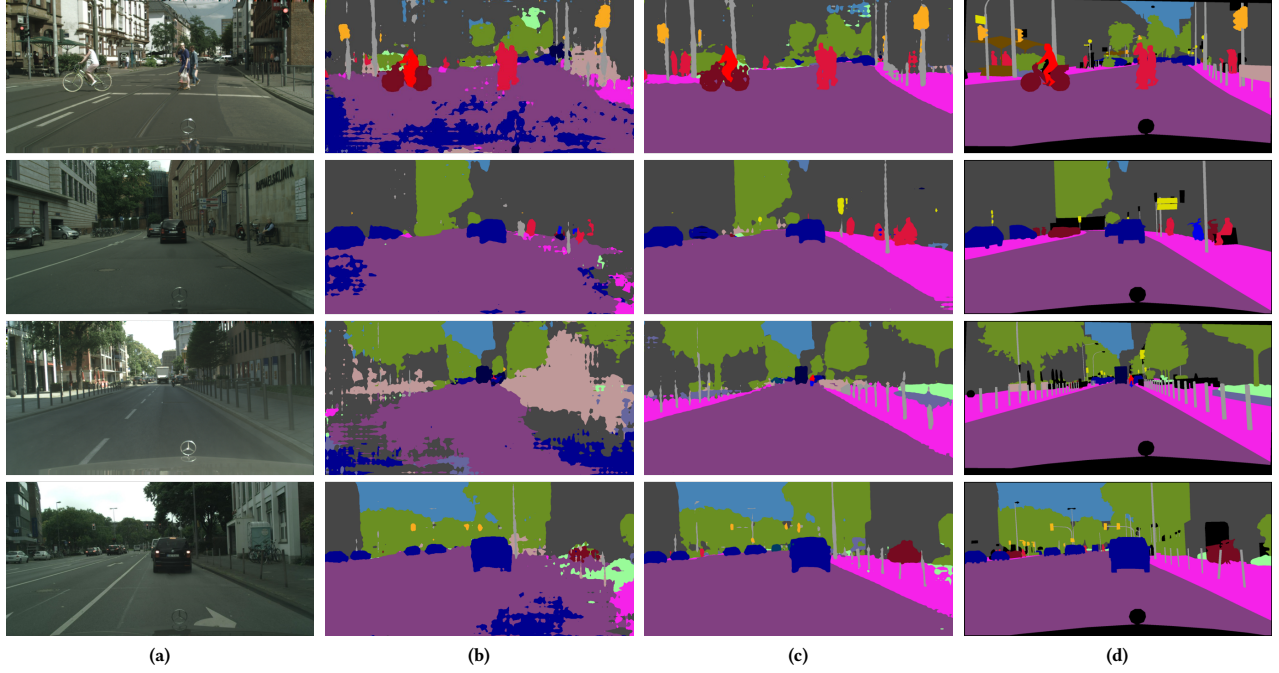


Figure 3: Qualitative results on the GTAV→Cityscapes task. (a) Input images from Cityscapes. (b) Segmentation results without domain adaptation. (c) Segmentation results of the proposed method. (d) Ground truth.

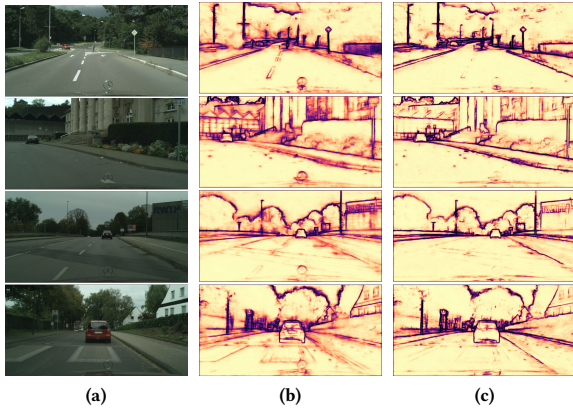


Figure 4: Illustrations of produced boundary maps. (a) Input images from Cityscapes. (b) Semantic boundary maps without adversarial learning. (c) Semantic boundary maps with adversarial learning.

outperform the model without domain adaptation (SourceOnly) by large performance margins. Then, our method has the best mIoU 52.8%, which is significantly better than that of the compared state-of-the-art methods. Compared with some adversarial training and self-supervised learning methods, such as CLAN and PyCDA, our method improves by 9.6% and 5.4% mIoU and has significant gains in almost all classes. Moreover, some methods also combine the

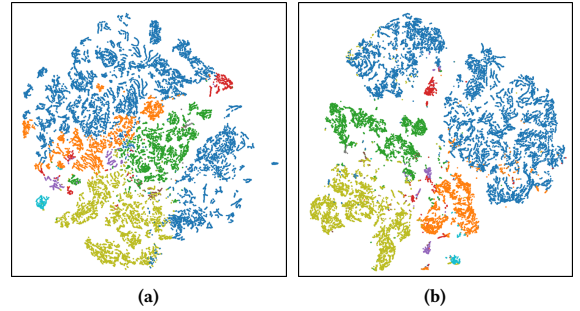


Figure 5: The t-SNE visualization of embedded semantic features over the target domain. (a) Features without the guide of edge information. (b) Features with the guide of edge information.

adversarial learning or image translation with self-supervised learning and achieve decent performance, like FDA, DAST, and UDACT. Compared to these methods, our approach still has a significant improvement. Figure 3 presents some qualitative results² produced by our methods.

SYNTHIA to Cityscapes. Table 2 reports the comparison results on the SYNTHIA→Cityscapes task. Like the previous work, we also report two mIoU metrics: 13 classes of mIoU* and 16 classes of mIoU. According to Table 2, it is obvious that our proposed method

²For more qualitative results, please see the supplementary materials.

Table 3: Ablation study of the proposed method in terms of mIoU (%) on the two tasks. Here, “Baseline” represents the original adversarial learning without entropy reweighting.

Baseline	\mathcal{L}_{sem}^{adv}	\mathcal{L}_{eq}^{con}	\mathcal{L}_{eq}^{adv}	\mathcal{L}_{uasl}	GTAV	SYNTHIA
✓					45.1	41.2
✓	✓				46.3	41.8
✓	✓	✓			48.4	43.7
✓	✓	✓	✓		49.2	44.4
✓	✓	✓	✓	✓	52.8	48.1

Table 4: Parameter analysis of the weighting factor α for the entropy reweighting adversarial loss in terms of mIoU (%).

GTAV→Cityscapes							
α	0	1	5	10	15	20	30
mIoU	45.1	45.2	45.8	46.3	46.0	45.3	43.0

Table 5: Comparison of the proposed UASL and standard self-supervised learning method with different thresholds T in terms of mIoU (%).

SL Type		GTAV	SYNTHIA
SL	$T = 0$	51.3	47.1
	$T = 0.5$	52.2	47.6
	$T = 0.9$	52.5	47.4
UASL		52.8	48.1

can outperform other state-of-the-art methods on both 13-class and 16-class with mIoU of 55.9% and 48.1%. In summary, these results obtained on both tasks reveal the effectiveness and superiority of our architecture in learning domain-invariant representations for UDA in semantic segmentation.

4.4 Discussion

We further report the ablation study results to demonstrate the performance contribution of each element in our proposed method in Table 3. It can be seen that each element contributes to the final success of the adaptation. The proposed method outperforms the “Baseline” by +7.7% and +6.9% with GTAV and SYNTHIA as the source, respectively.

Specifically, our proposed image-level entropy reweighting methods can enhance the model adaptation ability in the hard samples, thereby improving performance by 1.2% and 0.6%. Besides, weight factor α is an important parameter for the entropy reweighting adversarial loss, which controls the extra adaptation degree to hard samples, we evaluate the performance of the semantic stream with different α on the GTAV→Cityscapes task, as shown in Table 4. When $\alpha=0$, the loss is equal to the standard adversarial loss. As α increases, the loss of high-entropy samples (i.e., hard samples) is enlarged and hard samples could get better adaptation. However, if α is too large, the network could merely focus on the adaptation of

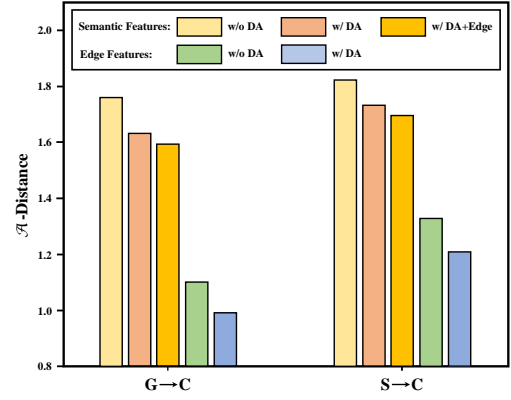


Figure 6: \mathcal{A} -distance of semantic and edge feature representations on the two tasks.

hard samples, which may damage the adaptation performance in easy samples.

Subsequently, utilizing low-level edge information can further enhance adaptation performance and lead to a large performance boost. Since the small domain gap in low-level edge features can be narrowed to some extent by semantic adversarial learning, using an independent edge stream to generate semantic boundaries and align the target prediction maps with them can improve mIoU by 2.1% and 1.9%. After explicitly performing adversarial learning for edge information, the mIoU get further improved by 0.8% and 0.7%. This obvious performance improvement (+2.9% and +2.6%) clearly demonstrates our argument. Figure 4 illustrates some produced semantic boundary maps. Obviously, through adversarial learning, the small inter-domain gap in edge features get further narrowed, thereby producing more accurate semantic boundaries. Then, in Figure 5, we additionally give a contrastive analysis between semantic feature distributions without and with the guide of edge information by t-SNE [40], which reveals that our edge consistency loss can enforce the alignment of semantic features, leading to clearer and more discriminative clusters over the target domain.

To further verify our argument, we display \mathcal{A} -distance [2] of semantic features and edge features in Figure 6, which is a commonly used metric for measuring domain discrepancy. Since it is difficult to compute the exact \mathcal{A} -distance, a proxy distance is defined as $\hat{d}_{\mathcal{A}} = 2(1 - 2\epsilon)$ [2], where ϵ is the generalization error of a classifier (SVM in this paper) trained on the binary problem of distinguishing samples between the source and target domains. From Figure 6, we could see that $\hat{d}_{\mathcal{A}}$ on edge features is obviously smaller than $\hat{d}_{\mathcal{A}}$ on semantic features, which proves that low-level edge information has a smaller inter-domain gap. After performing semantic adversarial learning, the $\hat{d}_{\mathcal{A}}$ on semantic features is reduced. Moreover, the $\hat{d}_{\mathcal{A}}$ on semantic features become smaller through the guide of edge information, which verifies that edge information can be explicitly used to facilitate the transfer of semantic information.

Lastly, through UASL, the mIoU performance of the proposed method reaches 52.8% and 48.1%. In addition, we also compare UASL to the standard SL method with three commonly used thresholds: $T = 0$ [32], $T = 0.5$ [27], and $T = 0.9$ [18]. The relevant results are

reported in Table 5. We could see that the threshold of generating pseudo-label significantly affects the performance of standard SL. And different domain adaptation tasks may have diverse optimal thresholds. It is difficult to choose a suitable threshold. In contrast, our UASL does not need to select a threshold. It can fully utilize target label information, adaptively pay large weights to high-confident pixels and suppress the effects of low-confident pixels, thereby obtaining better performance.

5 CONCLUSION

In this paper, we present a new domain adaptation approach by leveraging the low-level edge information that is easy to adapt to guide the transfer of high-level semantic information. Specifically, we propose a semantic-edge domain adaptation architecture. The semantic stream adopts the existing entropy adversarial learning approach. To better adapt hard target samples, an entropy reweighting method is presented to make the network pay more attention to hard samples. The edge stream can produce semantic boundaries. To make the target predicted boundaries more precise, adversarial learning is performed on the edge stream. For the purpose of explicitly guiding the transfer of semantic features, an edge consistency loss function is presented to ensure the consistency between the target semantic map and boundary map. Lastly, an uncertainty-adaptive self-supervised learning is proposed to further fit the distribution of the target domain. The experimental results in the two UDA segmentation scenarios from synthetic to real demonstrate that our method obtains better results than the existing state-of-the-art works.

REFERENCES

- [1] Vijay Badrinarayanan, Alex Kendall, and Roberto Cipolla. 2017. Segnet: A deep convolutional encoder-decoder architecture for image segmentation. *IEEE transactions on pattern analysis and machine intelligence* 39, 12 (2017), 2481–2495.
- [2] Shai Ben-David, John Blitzer, Koby Crammer, Fernando Pereira, et al. 2007. Analysis of representations for domain adaptation. *NIPS* 19 (2007), 137.
- [3] Maxim Berman, Amal Rannen Triki, and Matthew B Blaschko. 2018. The lovasz-softmax loss: A tractable surrogate for the optimization of the intersection-over-union measure in neural networks. In *CVPR*. 4413–4421.
- [4] Hongruiquan Chen, Chen Wu, Bo Du, and Liangpei Zhang. 2020. DSDANet: Deep Siamese Domain Adaptation Convolutional Neural Network for Cross-domain Change Detection. *arXiv preprint arXiv:2006.09225* (2020).
- [5] Hongruiquan Chen, Chen Wu, Bo Du, Liangpei Zhang, and Le Wang. 2020. Change Detection in Multisource VHR Images via Deep Siamese Convolutional Multiple-Layers Recurrent Neural Network. *IEEE Transactions on Geoscience and Remote Sensing* 58, 4 (2020), 2848–2864.
- [6] Liang-Chieh Chen, Jonathan T Barron, George Papandreou, Kevin Murphy, and Alan L Yuille. 2016. Semantic image segmentation with task-specific edge detection using cnns and a discriminatively trained domain transform. In *CVPR*. 4545–4554.
- [7] Liang-Chieh Chen, George Papandreou, Iasonas Kokkinos, Kevin Murphy, and Alan L Yuille. 2017. Deeplab: Semantic image segmentation with deep convolutional nets, atrous convolution, and fully connected crfs. *IEEE transactions on pattern analysis and machine intelligence* 40, 4 (2017), 834–848.
- [8] Jaehoon Choi, Taekyung Kim, and Changick Kim. 2019. Self-ensembling with gan-based data augmentation for domain adaptation in semantic segmentation. In *ICCV*. 6830–6840.
- [9] Marius Cordts, Mohamed Omran, Sebastian Ramos, Timo Rehfeld, Markus Endzweiler, Rodrigo Benenson, Uwe Franke, Stefan Roth, and Bernt Schiele. 2016. The cityscapes dataset for semantic urban scene understanding. In *CVPR*. 3213–3223.
- [10] Jifeng Dai, Kaiming He, and Jian Sun. 2016. Instance-aware semantic segmentation via multi-task network cascades. In *CVPR*. 3150–3158.
- [11] Jia Deng, Wei Dong, Richard Socher, Li-Jia Li, Kai Li, and Li Fei-Fei. 2009. Imagenet: A large-scale hierarchical image database. In *CVPR*. 248–255.
- [12] Zhangxuan Gu, Siyuan Zhou, Li Niu, Zihan Zhao, and Liqing Zhang. 2020. Context-aware Feature Generation for Zero-shot Semantic Segmentation. In *ACMMM*. 1921–1929.
- [13] Kaiming He, Xiangyu Zhang, Shaoqing Ren, and Jian Sun. 2016. Deep residual learning for image recognition. In *CVPR*. 770–778.
- [14] Judy Hoffman, Eric Tzeng, Taesung Park, Jun-Yan Zhu, Phillip Isola, Kate Saenko, Alexei Efros, and Trevor Darrell. 2018. Cycada: Cycle-consistent adversarial domain adaptation. In *ICML*. 1989–1998.
- [15] Judy Hoffman, Dequan Wang, Fisher Yu, and Trevor Darrell. 2016. Fcns in the wild: Pixel-level adversarial and constraint-based adaptation. *arXiv preprint arXiv:1612.02649* (2016).
- [16] Eric Jang, Shixiang Gu, and Ben Poole. 2016. Categorical reparameterization with gumbel-softmax. *arXiv preprint arXiv:1611.01144* (2016).
- [17] Junguang Jiang, Ximei Wang, Mingsheng Long, and Jianmin Wang. 2020. Re-source Efficient Domain Adaptation. In *ACMMM*. 2220–2228.
- [18] Myeongjin Kim and Hyeran Byun. 2020. Learning texture invariant representation for domain adaptation of semantic segmentation. In *CVPR*. 12975–12984.
- [19] Iasonas Kokkinos. 2017. Ubernet: Training a universal convolutional neural network for low-, mid-, and high-level vision using diverse datasets and limited memory. In *ICCV*. 6129–6138.
- [20] Vladlen Koltun et al. 2011. Efficient inference in fully connected crfs with gaussian edge potentials. *NIPS* 4 (2011).
- [21] Alex Krizhevsky, Ilya Sutskever, and Geoffrey E Hinton. 2012. Imagenet classification with deep convolutional neural networks. *NIPS* 25 (2012), 1097–1105.
- [22] Yann LeCun, Léon Bottou, Yoshua Bengio, and Patrick Haffner. 1998. Gradient-based learning applied to document recognition. *Proc. IEEE* 86, 11 (1998), 2278–2324.
- [23] Suhyeon Lee, Junhyuk Hyun, Hongje Seong, and Euntai Kim. 2021. Unsupervised Domain Adaptation for Semantic Segmentation by Content Transfer. In *AAAI*.
- [24] Guangrui Li, Guoliang Kang, Wu Liu, Yunchao Wei, and Yi Yang. 2020. Content-consistent matching for domain adaptive semantic segmentation. In *ECCV*. Springer, 440–456.
- [25] Shuang Li, Chi Harold Liu, Binhui Xie, Limin Su, Zhengming Ding, and Gao Huang. 2019. Joint adversarial domain adaptation. In *ACMMM*. 729–737.
- [26] Yunsheng Li, Lu Yuan, and Nuno Vasconcelos. 2019. Bidirectional learning for domain adaptation of semantic segmentation. In *CVPR*. 6936–6945.
- [27] Qing Lian, Fengmao Lv, Lixin Duan, and Boqing Gong. 2019. Constructing self-motivated pyramid curriculums for cross-domain semantic segmentation: A non-adversarial approach. In *ICCV*. 6758–6767.
- [28] Lizhao Liu, Junyi Cao, Minqian Liu, Yong Guo, Qi Chen, and Minghui Tan. 2020. Dynamic Extension Nets for Few-shot Semantic Segmentation. In *ACMMM*. 1441–1449.
- [29] Jonathan Long, Evan Shelhamer, and Trevor Darrell. 2015. Fully convolutional networks for semantic segmentation. In *CVPR*. 3431–3440.
- [30] Mingsheng Long, Yue Cao, Jianmin Wang, and Michael Jordan. 2015. Learning transferable features with deep adaptation networks. In *ICML*. PMLR, 97–105.
- [31] Yawei Luo, Liang Zheng, Tao Guan, Junqing Yu, and Yi Yang. 2019. Taking a closer look at domain shift: Category-level adversaries for semantics consistent domain adaptation. In *CVPR*. 2507–2516.
- [32] Fei Pan, Inkyu Shin, Francois Rameau, Seokju Lee, and In So Kweon. 2020. Un-supervised Intra-domain Adaptation for Semantic Segmentation through Self-Supervision. In *CVPR*. 3764–3773.
- [33] Dzong L Pham, Chenyang Xu, and Jerry L Prince. 2000. Current methods in medical image segmentation. *Annual review of biomedical engineering* 2, 1 (2000), 315–337.
- [34] Stephan R Richter, Vibhav Vineet, Stefan Roth, and Vladlen Koltun. 2016. Playing for data: Ground truth from computer games. In *ECCV*. 102–118.
- [35] German Ros, Laura Sellart, Joanna Materzynska, David Vazquez, and Antonio M Lopez. 2016. The synthia dataset: A large collection of synthetic images for semantic segmentation of urban scenes. In *CVPR*. 3234–3243.
- [36] Liangchen Song, Yonghao Xu, Lefei Zhang, Bo Du, Qian Zhang, and Xinggang Wang. 2020. Learning from synthetic images via active pseudo-labeling. *IEEE Transactions on Image Processing* 29 (2020), 6452–6465.
- [37] Towaki Takikawa, David Acuna, Varun Jampani, and Sanja Fidler. 2019. Gated-scnn: Gated shape cnns for semantic segmentation. In *ICCV*. 5229–5238.
- [38] Yi-Hsuan Tsai, Wei-Chih Hung, Samuel Schuster, Kihyuk Sohn, Ming-Hsuan Yang, and Manmohan Chandraker. 2018. Learning to adapt structured output space for semantic segmentation. In *CVPR*. 7472–7481.
- [39] Yi-Hsuan Tsai, Kihyuk Sohn, Samuel Schuster, and Manmohan Chandraker. 2019. Domain adaptation for structured output via discriminative patch representations. In *ICCV*. 1456–1465.
- [40] Laurens Van der Maaten and Geoffrey Hinton. 2008. Visualizing data using t-SNE. *Journal of machine learning research* 9, 11 (2008).
- [41] Tuan-Hung Vu, Himalaya Jain, Maxime Bucher, Matthieu Cord, and Patrick Pérez. 2019. Advent: Adversarial entropy minimization for domain adaptation in semantic segmentation. In *CVPR*. 2517–2526.
- [42] Tuan-Hung Vu, Himalaya Jain, Maxime Bucher, Matthieu Cord, and Patrick Pérez. 2019. Dada: Depth-aware domain adaptation in semantic segmentation. In *ICCV*. 7364–7373.

- [43] Haoran Wang, Tong Shen, Wei Zhang, Ling-Yu Duan, and Tao Mei. 2020. Classes Matter: A Fine-grained Adversarial Approach to Cross-domain Semantic Segmentation. In *ECCV*. Springer, 642–659.
- [44] Limin Wang, Yuanjun Xiong, Zhe Wang, Yu Qiao, Dahua Lin, Xiaoou Tang, and Luc Van Gool. 2016. Temporal segment networks: Towards good practices for deep action recognition. In *ECCV*. 20–36.
- [45] Yuhang Wang, Jing Liu, Yong Li, Junjie Yan, and Hanqing Lu. 2016. Objectness-aware semantic segmentation. In *ACMMM*. 307–311.
- [46] Chen Wu, Hongruixuan Chen, Bo Du, and Liangpei Zhang. 2021. Unsupervised Change Detection in Multitemporal VHR Images Based on Deep Kernel PCA Convolutional Mapping Network. *IEEE Transactions on Cybernetics* (2021), 1–15.
- [47] Hai Xu, Hongtao Xie, Zheng-Jun Zha, Sun-ao Liu, and Yongdong Zhang. 2020. March on Data Imperfections: Domain Division and Domain Generalization for Semantic Segmentation. In *ACMMM*. 3044–3053.
- [48] Yonghao Xu, Bo Du, Lefei Zhang, Qian Zhang, Guoli Wang, and Liangpei Zhang. 2019. Self-ensembling attention networks: Addressing domain shift for semantic segmentation. In *AAAI*, Vol. 33. 5581–5588.
- [49] Jinyu Yang, Weizhi An, Sheng Wang, Xinliang Zhu, Chaochao Yan, and Junzhou Huang. 2020. Label-driven reconstruction for domain adaptation in semantic segmentation. In *ECCV*. Springer, 480–498.
- [50] Yanchao Yang and Stefano Soatto. 2020. Fda: Fourier domain adaptation for semantic segmentation. In *CVPR*. 4085–4095.
- [51] Fei Yu, Mo Zhang, Hexin Dong, Sheng Hu, Bin Dong, and Li Zhang. 2021. DAST: Unsupervised Domain Adaptation in Semantic Segmentation Based on Discriminator Attention and Self-Training. In *AAAI*.
- [52] Matthew D Zeiler and Rob Fergus. 2014. Visualizing and understanding convolutional networks. In *ECCV*. Springer, 818–833.
- [53] Yang Zhang, Philip David, Hassan Foroosh, and Boqing Gong. 2019. A curriculum domain adaptation approach to the semantic segmentation of urban scenes. *IEEE transactions on pattern analysis and machine intelligence* 42, 8 (2019), 1823–1841.
- [54] Yiheng Zhang, Zhaofan Qiu, Ting Yao, Dong Liu, and Tao Mei. 2018. Fully convolutional adaptation networks for semantic segmentation. In *CVPR*. 6810–6818.
- [55] Ziyu Zhang, Sanja Fidler, and Raquel Urtasun. 2016. Instance-level segmentation for autonomous driving with deep densely connected mrfs. In *CVPR*. 669–677.
- [56] Hengshuang Zhao, Jianping Shi, Xiaojuan Qi, Xiaogang Wang, and Jiaya Jia. 2017. Pyramid scene parsing network. In *CVPR*. 2881–2890.
- [57] Jun-Yan Zhu, Taesung Park, Phillip Isola, and Alexei A Efros. 2017. Unpaired image-to-image translation using cycle-consistent adversarial networks. In *ICCV*. 2223–2232.
- [58] Junbao Zhuo, Shuhui Wang, Weigang Zhang, and Qingming Huang. 2017. Deep unsupervised convolutional domain adaptation. In *ACMMM*. 261–269.
- [59] Danbing Zou, Qikui Zhu, and Pingkun Yan. 2020. Unsupervised domain adaptation with dual-scheme fusion network for medical image segmentation. In *IJCAI*. 3291–3298.
- [60] Yang Zou, Zhiding Yu, BVK Vijaya Kumar, and Jinsong Wang. 2018. Unsupervised domain adaptation for semantic segmentation via class-balanced self-training. In *ECCV*. 289–305.